"Long baseline neutrino experiments and quasi-elastic neutrino charged current scattering off nucleus"

Anatoli Butkevich (INR RAS)

RAS Conference " Physics of fundamental interactions", IHEP, Protvino, December 23, 2008

- Long baseline neutrino experiments and their goals.
  - ($\star$) Precise measurements of the neutrino mass squared differences Δm^2_{23} ($\delta\Delta m^2_{23}/\Delta m^2_{23} \leq 10\%$) through muon neutrino disappearance measurements (K2K, MINOS, T2K).
  - ($\star$) Search for the last unmeasured leptonic mixing angle θ_{13} through muon to electron neutrino transition (T2K, NOvA).
  - ($\star$) Search for CP violation with may be large in leptonic sector.
  - ($\star$) Determing the neutrino mass hierarchy to see if neutrino masses are organized the way as the charged fermions.
- Neutrino Beamline.
  - ($\star$) Neutrino beam spectra with mean neutrino energies $0.7 \leq \varepsilon_\nu \leq 3.5$ GeV.
  - ($\star$) Distance between the neutrino source and neutrino detectors $250 \leq \ L \leq 800$ km.

Measuring the Δm^2.

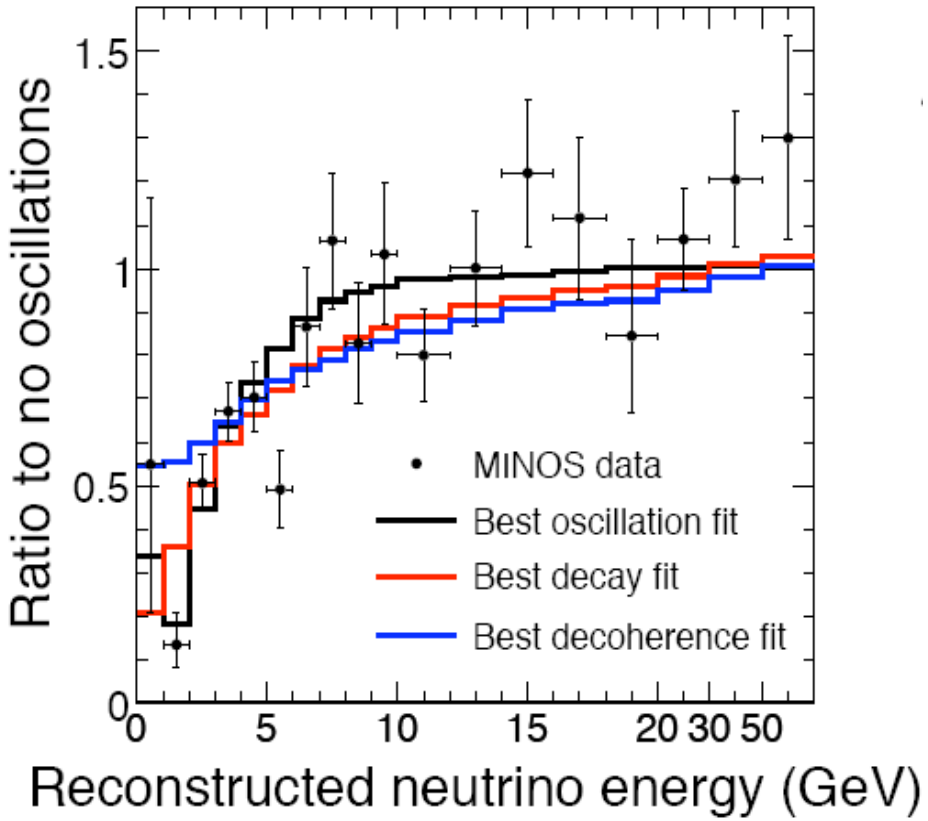

Observed dependence of the survival probability of neutrinos as a function of the neutrino energy.

$$P(\nu_\mu \to \nu_\mu) = 1 - \sin^2 2\theta \sin^2 \frac{1.27\Delta m^2(eV^2)L(km)}{\varepsilon_\nu(GeV)}$$

Position of the minimum ε_{min} yields the value of Δm^2

$$\Delta m^2 = \frac{\pi}{2} \cdot \frac{\varepsilon_{min}}{1.27L}$$

http://www-numi.fnal.gov/PublicInfo/forscientists.html

Measuring the neutrino energy.

1. Kinematic method for detectors (Cherenkov detectors) with the energy threshold for proton detection $\varepsilon_{th} \geq 1$ GeV.

($\star$) Selection of the charged current quasi-elastic (CCQE) one-track events
($\star$) Reconstruction the muon momentum (energy) $k_\mu(\varepsilon_\mu)$ and scattering angle θ and using

$$\varepsilon_\nu = (\varepsilon_\mu M - m_\mu^2)/(M + k_\mu \cos\theta - \varepsilon_\mu)$$

($\star$) Main sources of the systematic errors are: nonCCQE events and nucleon Fermi motion.
($\star$) 2. Calorimetrical method for detectors with low energy threshold for pion and proton detection

$$\varepsilon_\nu = \varepsilon_\mu + T_{had},$$

where T_{had} is the kinetic energy of the hadron final state.
($\star$) Systematic errors increases with multiplicity of the final state particles.

Strategies for Near Detector design.

($\star$) Systematic uncertainties on the incident neutrino flux, the neutrino interaction model, and the effects of the detector on the neutrino events selection and energy reconstruction will be dominate.
($\star$) Near detectors is as similar as possible to the far detector.
($\star$) Near detectors is much more segmented and fine grained.

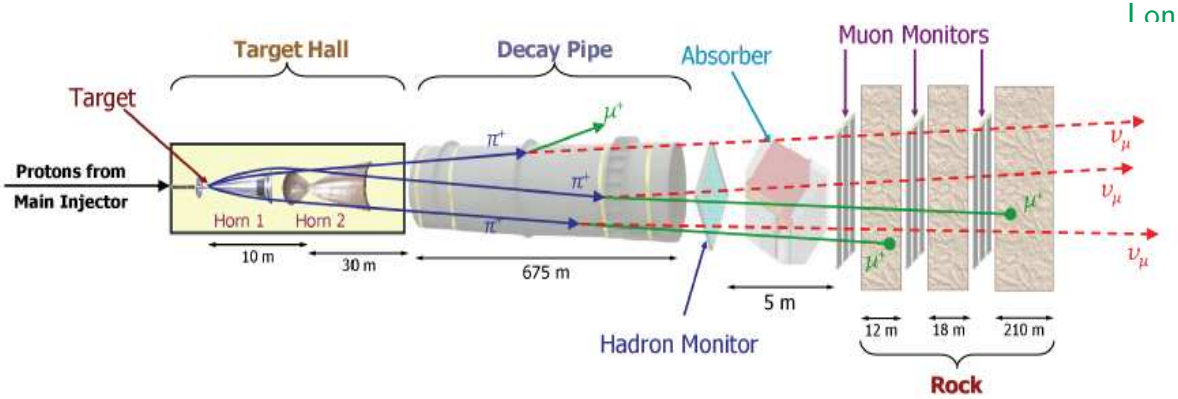
Target Hall
Decay Pipe
Absorber
Muon Monitors
Target
Protons from
Main Injector
Horn 1
Horn 2
10 m
30 m
675 m
5 m
12 m
18 m
210 m
Hadron Monitor
Rock


Soudan
Duluth
MN
WI
Lake Superior
Lake Michigan
Madison
MI
IA
Fermilab
IL
IN
MO


Fermilab
10 km
Soudan
12 km
735
km
1 kton
5.4 kton

The Monte Carlo simulation of the detector response to neutrino interaction and nuclear models for neutrino scattering off nuclei.

The most part of neutrino event generators are based on the Relativistic Fermi Gas Model (RFGM).

- ($\star$) Flat nucleon momentum distribution up to the Fermi momentum p_F and nuclear binding energy ϵ_b with Pauli blocking.
- ($\star$) RFGM does not take into account the nuclear shell structure, final state interaction (FSI), and the presence of short-range nucleon-nucleon NN correlation.
- ($\star$) The accuracy of the RFGM prediction becomes poor at low Q^2 and this model fails off in application to the exclusive cross sections (eA-data: JLab,Saclay,NIKHEF,Frascaty, νA-data: K2K,MiniBooNe.)

The Relativistic Distorted-Wave Impulse Approximation (was pioneered by A. Picklesimer et al. (1985,1987,1989) and developed in more detail by several groups [J.Udias et al. (1993), J.P.McDermott et al. (1991), Y.Jin et al. (1992), M.Hedayati-Poor et al. (1995) J.J.Kelly (1999), A.Meucci et al (2001)])

- ($\star$) The RDWIA takes into account the nuclear shell structure and FSI effects.
- ($\star$) The RDWIA was successfully tested against the data for eA scattering.

Electron and neutrino scattering off nuclei are closely interconnected and one can treat both processes within the same formalism.

($\star$) The RDWIA approach as well as Plane-Wave Impulse Approximation (PWIA) (the FSI effects are neglected) were applied to the neutrino-nucleus interaction for calculation the CCQE cross sections. The FSI effects on the inclusive and total cross sections in the presence of the NN correlations were estimated.

For more details of the present approach see:
A.Butkevich, S.Mikheyev,Phys.Rev.C72:025501,2005;
A.Butkevich, S.Kulagin,Phys.Rev.C76:045502,2007;
A.Butkevich,Phys.Rev.C78:015501,2008

Cross sections

Lepton CC QE exclusive reaction

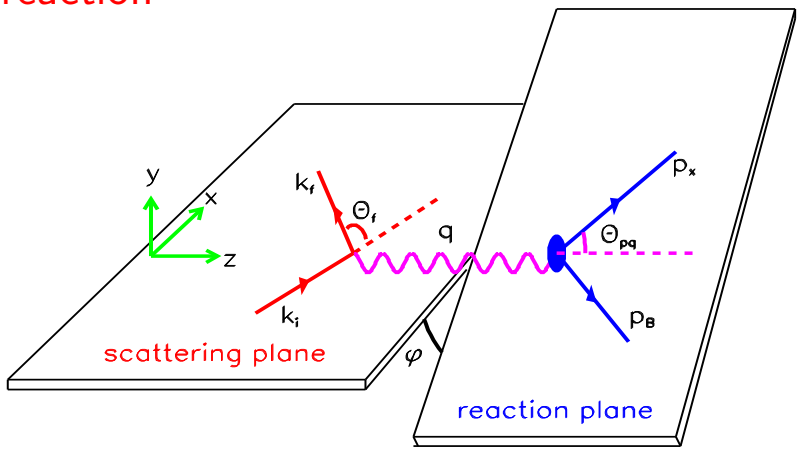

$$\frac{d^5\sigma^{el}}{d\varepsilon_f d\Omega_f d\Omega_x} = R\frac{|\boldsymbol{p}_x|\varepsilon_x}{(2\pi)^3}\frac{\varepsilon_f}{\varepsilon_i}\frac{\alpha^2}{Q^4}L^{(el)}_{\mu\nu}W^{\mu\nu(el)}$$

$$\frac{d^5\sigma^{cc}}{d\varepsilon_f d\Omega_f d\Omega_x} = R\frac{|\boldsymbol{p}_x|\varepsilon_x}{(2\pi)^5}\frac{|\boldsymbol{k}_f|}{\varepsilon_i}\frac{G^2\cos^2\theta_c}{2}L^{(cc)}_{\mu\nu}W^{\mu\nu(cc)},$$

where R is a recoil factor

$$R = \left|1 - \frac{\varepsilon_x}{\varepsilon_B}\frac{\boldsymbol{p}_x\cdot\boldsymbol{p}_B}{\boldsymbol{p}_x\cdot\boldsymbol{p}_x}\right|^{-1},$$

$L^{(cc)}_{\mu\nu}$ and $W^{\mu\nu(cc)}$ are lepton and hadronic tensors, ε_f, Ω_f are energy and solid angle of the scattered lepton, Ω_x is solid angle for ejectile nucleon momentum,

$G \simeq 1.16639 \times 10^{-11}$ MeV^{-2} is the Fermi constant, θ_C is the Cabbibo angle ($\cos\theta_C \approx 0.9749$), $\alpha \simeq 1/137$ is the fine-structure constant. A useful quantity to compare nuclear calculations for electron and neutrino scattering is reduced cross section

$$\sigma_{red} = \frac{d^5\sigma}{d\varepsilon_f d\Omega_f d\Omega_x} / K\sigma_{lN},$$

where $K^{el} = Rp_x\varepsilon_x/(2\pi)^3$ and $K^{cc} = Rp_x\varepsilon_x/(2\pi)^5$ are phase-space factors for electron and neutrino scattering and σ_{lN} is elementary cross section for the lepton scattering from moving free nucleon.

- The lepton tensor can be written as the sum of symmetric $L_S^{\mu\nu}$ and antisymmetric $L_A^{\mu\nu}$ tensors

$$L^{\mu\nu} = L_S^{\mu\nu} + L_A^{\mu\nu}$$
$$L_S^{\mu\nu} = 2\left(k_i^\mu k_f^\nu + k_i^\nu k_f^\mu - g^{\mu\nu} k_i k_f\right)$$
$$L_A^{\mu\nu} = h2i\epsilon^{\mu\nu\alpha\beta}(k_i)_\alpha (k_f)_\beta,$$

  where h is $+1$ for positive lepton helicity and -1 for negative lepton helicity, $\epsilon^{\mu\nu\alpha\beta}$ is the antisymmetric tensor

- The electromagnetic and weak CC hadronic tensors $W_{\mu\nu}^{(el)(cc)}$ is given by bilinear products of the transition matrix elements of the nuclear CC operator $J_{\mu}^{(el)(cc)}$ between the initial nucleus state $|A\rangle$ and the final state $|B_f\rangle$ as

$$W_{\mu\nu}^{(el)(cc)} = \sum_f \langle B_f, p_x | J_{\mu}^{(el)(cc)} | A \rangle \langle A | J_{\nu}^{(el)(cc)\dagger} | B_f, p_x \rangle$$

  where the sum is taken over undetected states.
- In the inclusive reactions only the outgoing lepton is detected and the differential cross sections can be written as

$$\frac{d^3\sigma}{d\varepsilon_f d\Omega_f} = \frac{1}{(2\pi)^2} \frac{|\boldsymbol{k}_f|}{\varepsilon_i} \frac{G^2 \cos^2\theta_c}{2} L_{\mu\nu} \mathcal{W}^{\mu\nu},$$

  where $\mathcal{W}^{\mu\nu}$ is inclusive hadronic tensor.

- We describe the lepton-nucleon scattering in the Impulse Approximation (IA), in which only one nucleon of the target is involved in reaction and the nuclear current is written as the sum of single-nucleon currents. Then, the nuclear matrix element takes the form

$$\langle p, B | J^{\mu} | A \rangle = \int d^3r \ \exp(i\boldsymbol{t}\cdot\boldsymbol{r}) \overline{\Psi}^{(-)}(\boldsymbol{p},\boldsymbol{r}) \Gamma^{\mu} \Phi(\boldsymbol{r}),$$

  where Γ^{μ} is the vertex function, $\boldsymbol{t} = \varepsilon_B \boldsymbol{q}/W$ is the recoil-corrected momentum transfer,

$W = \sqrt{(m_A + \omega)^2 - \boldsymbol{q}^2}$ is the invariant mass, Φ and $\Psi^{(-)}$ are relativistic bound-state and outgoing wave functions.

- Most calculations use the CC2 electromagnetic vertex function.

$$\Gamma^{\mu(el)} = F_V^{(el)}(Q^2)\gamma^\mu + i\sigma^{\mu\nu}\frac{q_\nu}{2m}F_M^{(el)}(Q^2),$$

where $\sigma^{\mu\nu} = i[\gamma^\mu\gamma^\nu]/2$, $F_V^{(el)}$ and $F_M^{(el)}$ are the Dirac and Pauli nucleon form factors.

- The single-nucleon charged current has $V-A$ structure $J^\mu = J_V^\mu + J_A^\mu$. For a free nucleon vertex function $\Gamma^\mu = \Gamma_V^\mu + \Gamma_A^\mu$ we use CC2 vector current vertex function

$$\Gamma_V^\mu = F_V(Q^2)\gamma^\mu + i\sigma^{\mu\nu}\frac{q_\nu}{2m}F_M(Q^2)$$

and the axial current vertex function

$$\Gamma_A^\mu = F_A(Q^2)\gamma^\mu\gamma_5 + F_P(Q^2)q^\mu\gamma_5.$$

We use the MMD approximation [P.Mergell et al (1996)] of the nucleon form factors.

- The axial F_A and psevdoscalar F_P form factors in the dipole approximation

$$F_A(Q^2) = \frac{F_A(0)}{(1 + Q^2/M_A^2)^2}, \quad F_P(Q^2) = \frac{2mF_A(Q^2)}{m_\pi^2 + Q^2},$$

where $F_A(0) = 1.267$, m_π is the pion mass, and $M_A \simeq 1.032$ GeV is the axial mass.

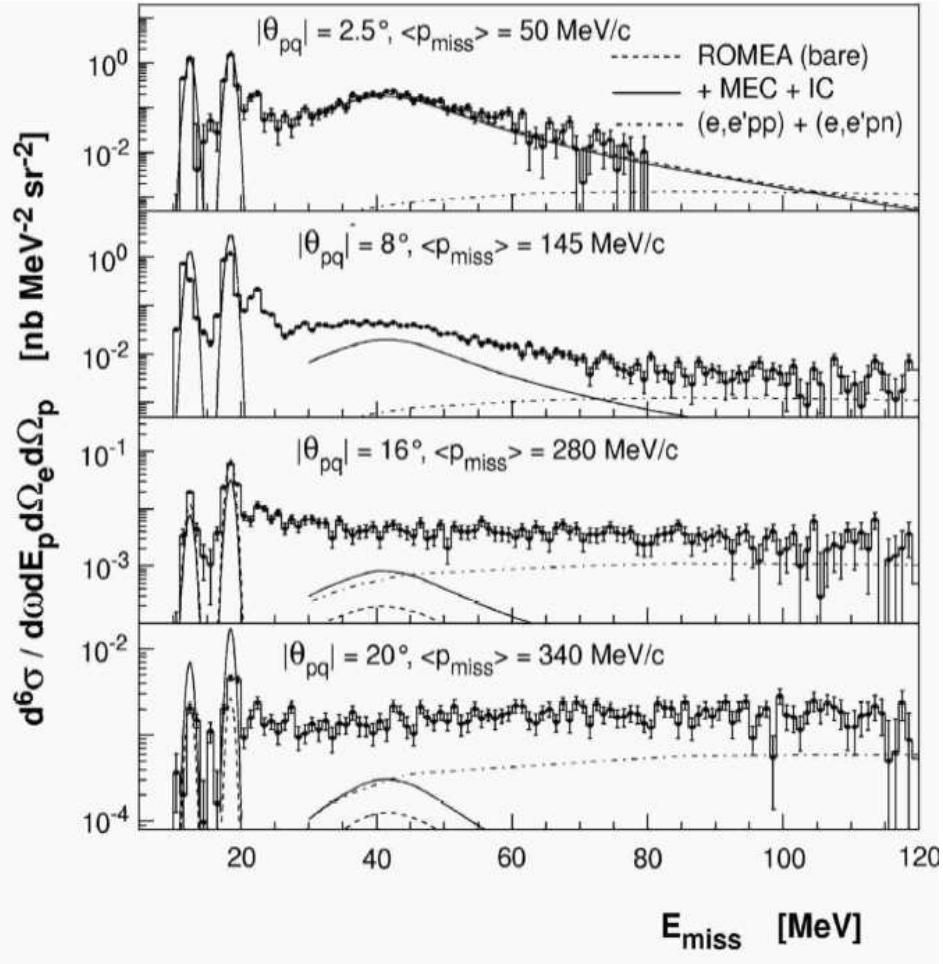

Bound-state wave function

Shell occupancy for Oxygen:

$S(P_{1/2})$=0.7

$S(P_{3/2})$=0.66

$S(S_{1/2})$=1

Average occupancy of nuclear shells $\overline{S}$=0.75 [supported by JLab measurement K. G. Fissum et al. (2005)]

Missing Energy

Neutron: 15.7 MeV $(1p_{1/2})$,
21.2 MeV $(1p_{3/2})$,
42.9 MeV $(1s_{1/2})$

Proton: $E_m(1p_{1/2})$=12.1 MeV,
$E_m(1p_{3/2})$=18.4 MeV,
$E_m(1s_{1/2})$=40.1 MeV

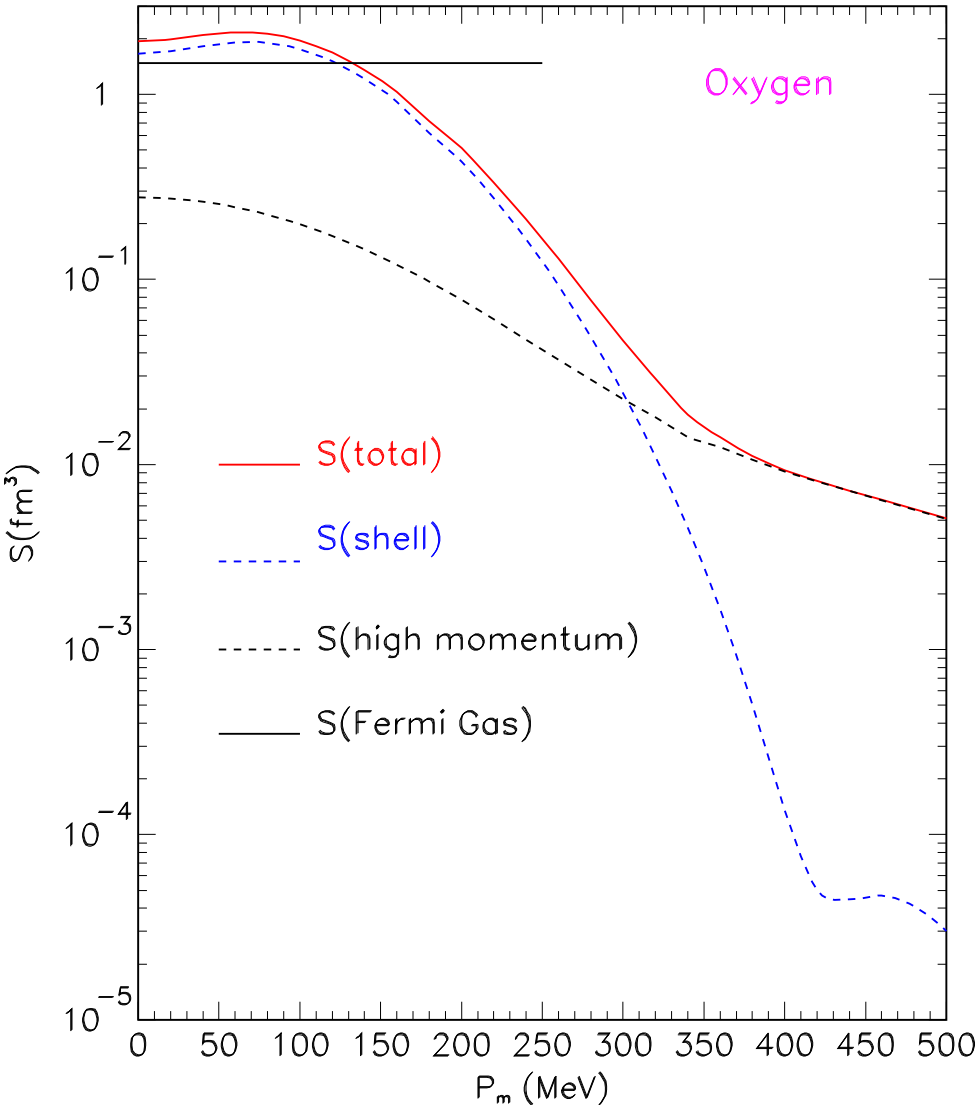

Bound-state wave function Φ

In independ particle shell model the relativistic bound-state functions of the shell nucleons Φ are obtained within the Hartree–Bogolioubov approximation in the $\sigma - \omega$ model (mean field wave functions) [B.Serot et al. 1986].

According to JLab data [K. Fissum (2004)] the occupancy of the IPSM orbitals of ^{16}O is approximately 75% on average. We consider a phenomenological model in PWIA, which incorporates high-energy and high-momentum component P_{HM} due to NN-correlations [C.Ciofi degli Atti et al (1996), S.Kulagin et al (2006)].

In our calculations the spectral function P_{HM} incorporates 25% of the total normalization of the spectral function.

Outgoing state wave functions

- In the RDWIA the final state interaction between the outgoing nucleon and the residual nucleus is taking into account and the ejectile wave function Ψ is solution of a Schrödinger equation containing equivalent central and spin-orbit potentials, which are functions of the scalar and vector potentials S and V, and are energy dependent.

- We use the LEA program [J.J. Kelly (1995)] for numerical calculation of the distorted wave functions with EDAD1 SV relativistic optical potential [E. Cooper (1993)].

- In the PWIA the final state interaction between the outgoing nucleon and the residual nucleus is neglected and the ejectile wave function Ψ is plane wave.

- In Fermi Gas model for oxygen we use p_F=250 MeV/c and ε=27 MeV. The RFGM does not account nuclear shell structure, FSI effect, and the presence of NN-correlations.

Inclusive cross section and missing flux problem

- For inclusive reaction (sum over all channels) probability flux must conserve.
- We calculate the contribution to inclusive and total cross sections for nuclear shells using only the real part of optical potential.
- We also apply FSI correction to the contribution from the high-momentum part of nuclear spectral function

$$\frac{d^3\sigma}{d\varepsilon_f d\Omega_f} = \underbrace{\left(\frac{d^3\sigma}{d\varepsilon_f d\Omega_f}\right)_{RDWIA}}_{nuclear\ \ shells} + \Lambda(\varepsilon_f, \Omega_f) \underbrace{\left(\frac{d^3\sigma}{d\varepsilon_f d\Omega_f}\right)_{HM}}_{NN\ \ correlations},$$

where

$$\Lambda(\varepsilon_f, \Omega_f) = \underbrace{\left(\frac{d^3\sigma}{d\varepsilon_f d\Omega_f}\right)_{RDWIA}}_{nuclear\ \ shells} \Big/ \underbrace{\left(\frac{d^3\sigma}{d\varepsilon_f d\Omega_f}\right)_{PWIA}}_{nuclear\ \ shells},$$

describes the relative strength of FSI.

More details about calculation can be found in NPA 766:142,2006 and PRC 76:045502,2007.

Analysis and Results

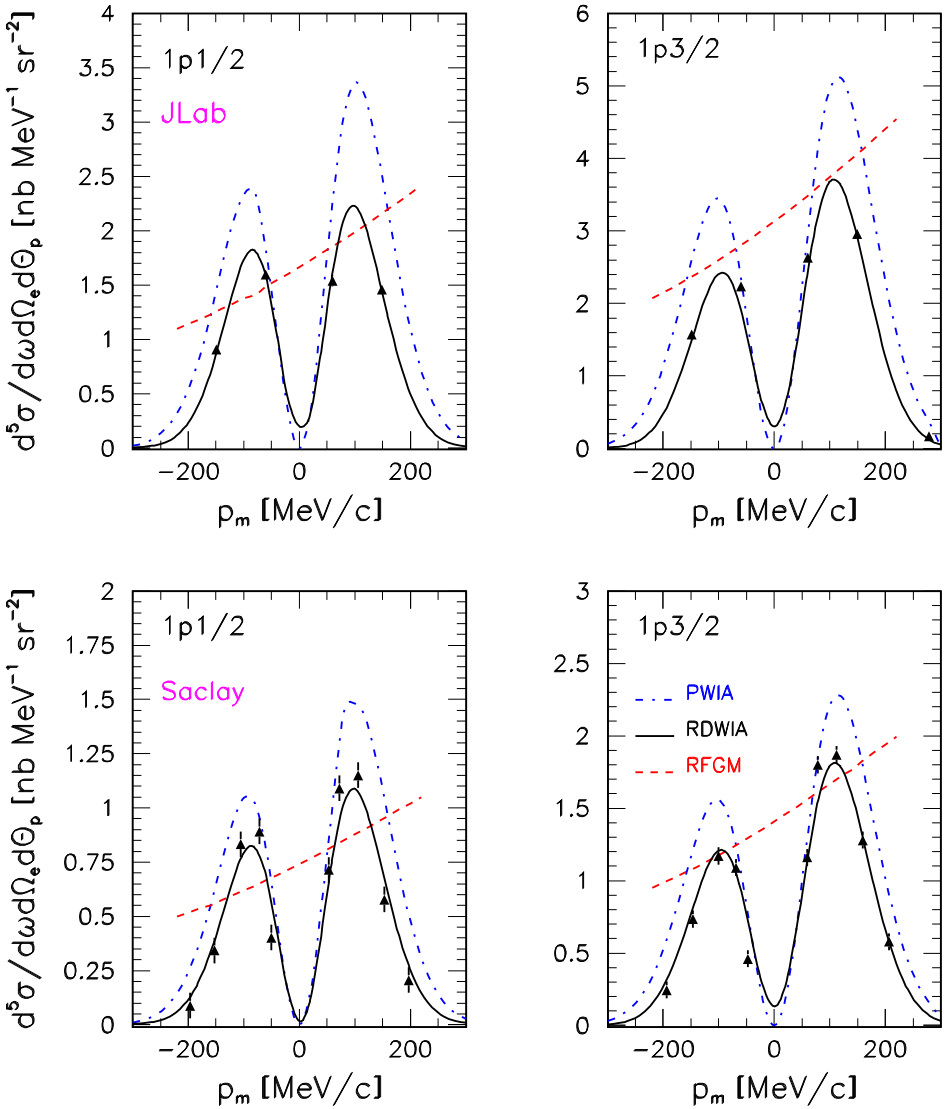

Measured differential exclusive cross section data for the removal of protons from 1p-shell of ^{16}O as a function of missing momentum . The upper panels show JLab data for electron beam energy E_{beam}=2.442 GeV, proton kinetic energy T_p=427 MeV, and Q^2=0.8 GeV^2. The lower panels show Saclay data for E_{beam}=580 MeV, T_p=160 MeV, and Q^2=0.3 GeV^2. The solid line is the RDWIA calculation while the dashed-dotted and dashed lines are respectively the PWIA and RFGM calculations. Negative values of p_m correspond to $\phi = \pi$ and positive ones to $\phi = 0$.

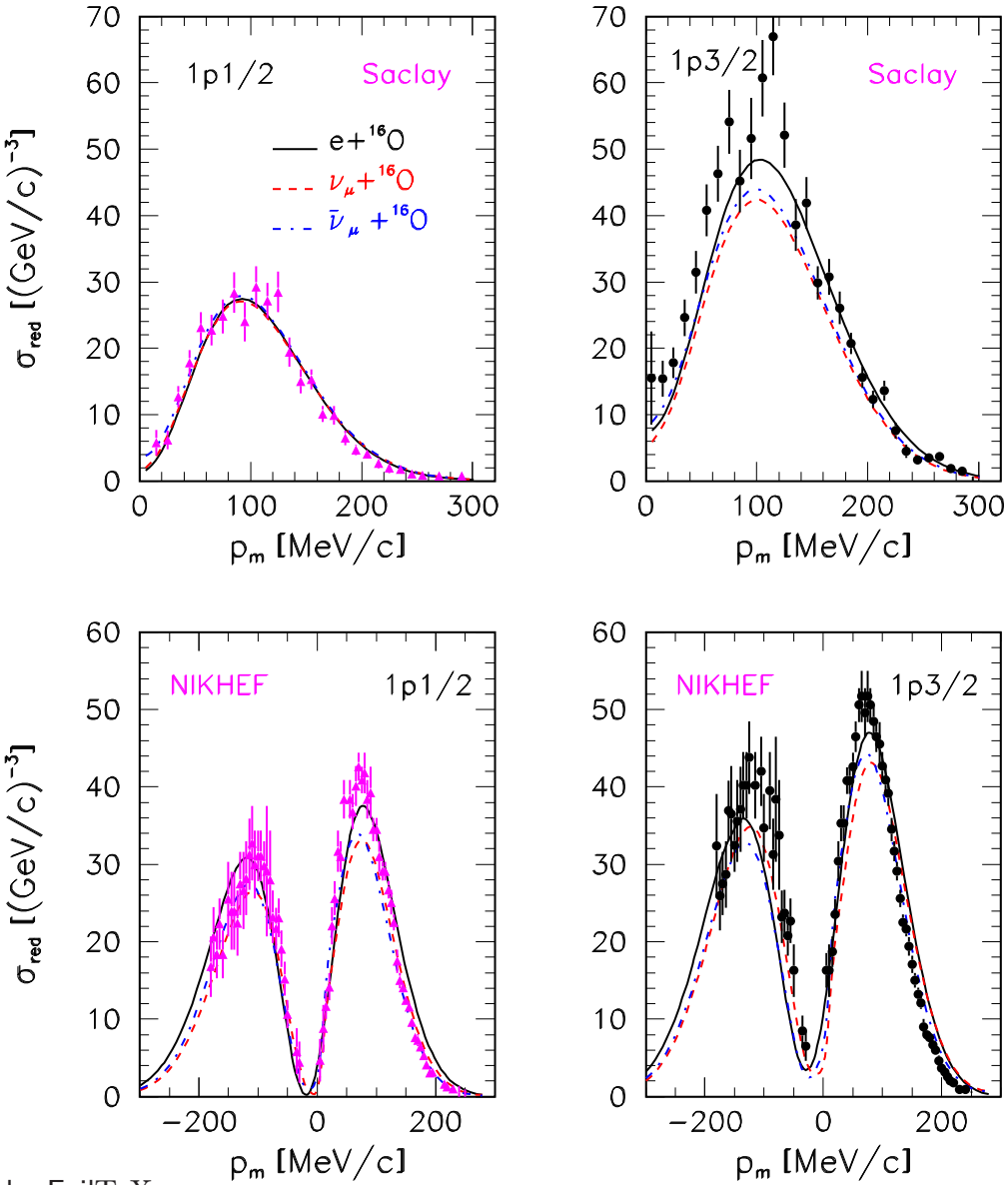

Comparison of the RDWIA electron, neutrino and antineutrino reduced cross sections for the removal of nucleons from 1p-shell of ^{16}O for Saclay (upper panels) and NIKHEF (lower panels) kinematic as functions of p_m. The solid line is electron while the dashed and dashed-dotted lines are respectively neutrino and antineutrino cross sections.

At the maximum electron cross section are higher (less than 10%) than (anti)neutrino ones.

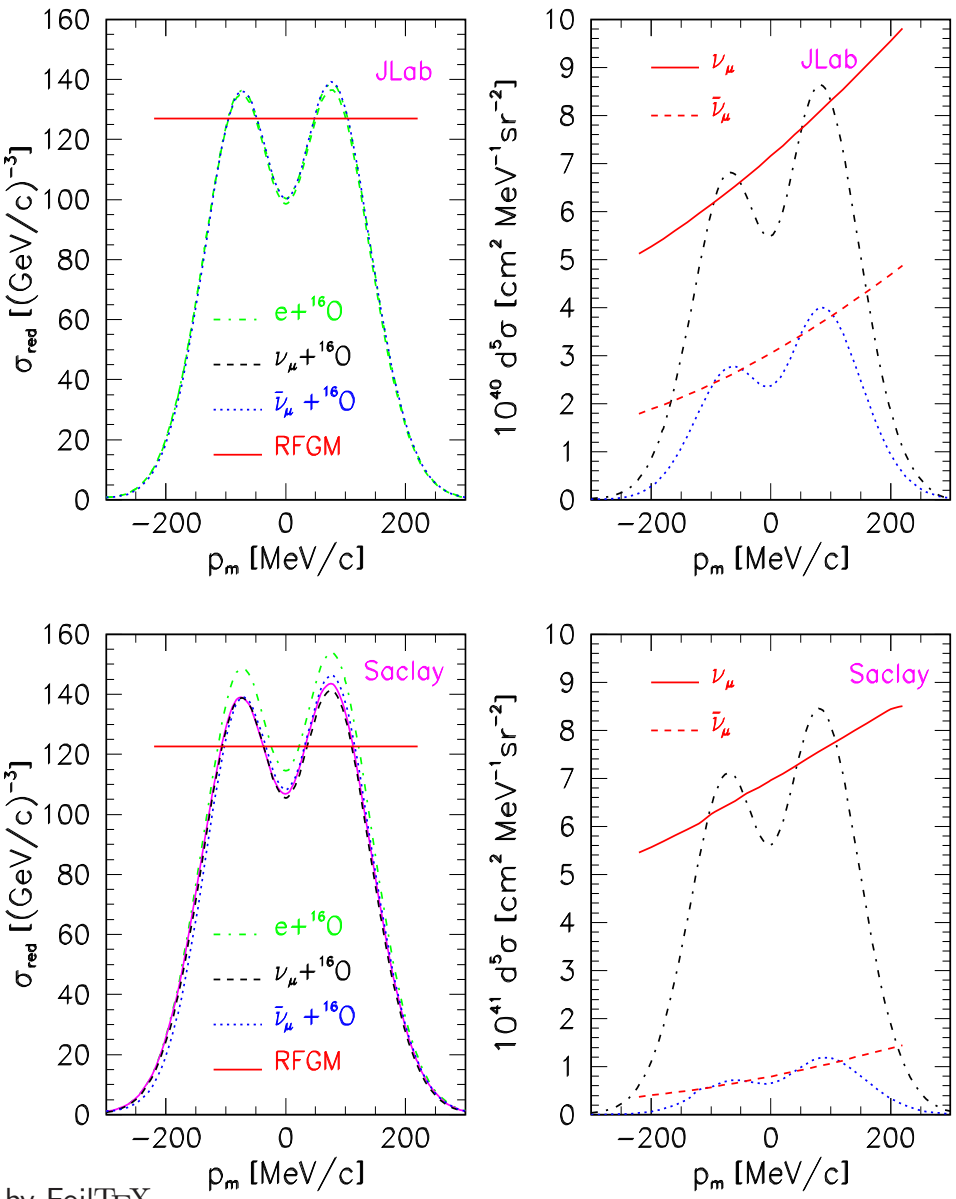

Comparison of the RDWIA and the RFGM calculations for electron, neutrino and antineutrino reduced and differential results for the removal of nucleons from 1p- and 1s-shells of ^{16}O. The dashed-dotted line is the RDWIA calculation for electron scattering while the dashed and dotted lines are respectively for neutrino and antineutrino scattering. The solid line on the left panels shows the RFGM result while the solid and dashed lines on the right panels are respectively neutrino and antineutrino cross sections calculated in the Fermi gas model. The dashed-dotted and dotted lines on right panels are respectively neutrino and antineutrino cross sections calculated in the RDWIA.

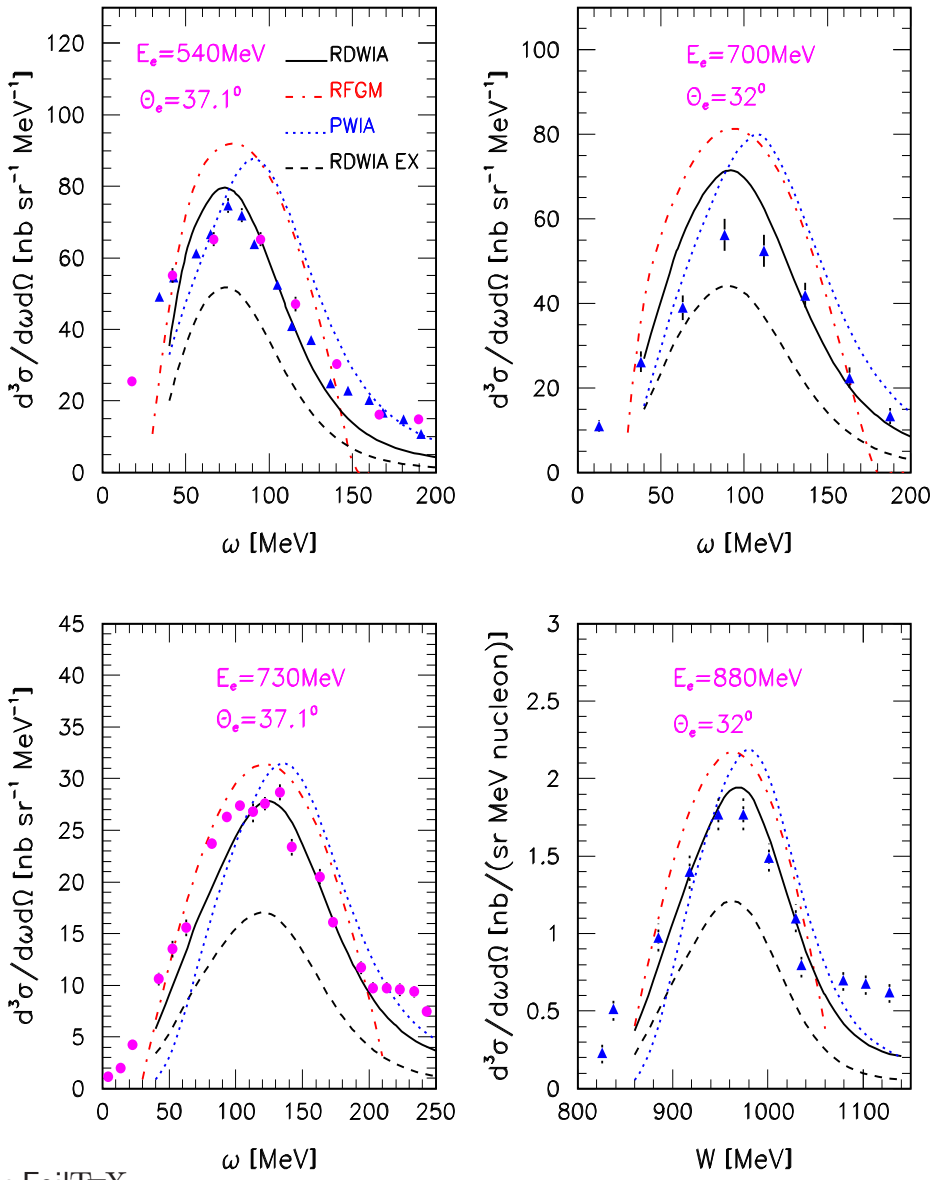

Inclusive cross section versus the energy transfer ω or invariant mass W (lower-right panel) for electron scattering on ^{16}O. The data are from SLAC (filled circles) and Frascati filled triangles). SLAC data are for electron beam energy E_e=540, 730 MeV and scattering angle θ=37.1°. Frascati data are for E_e=540 MeV and θ=37.1°, E_e=700, 880 MeV and θ=32°. The solid line is the RDWIA calculation while the dotted and dashed-dotted lines are respectively the PWIA and RFGM calculations. The dashed line is the cross section calculated in the RDWIA with complex optical potential.

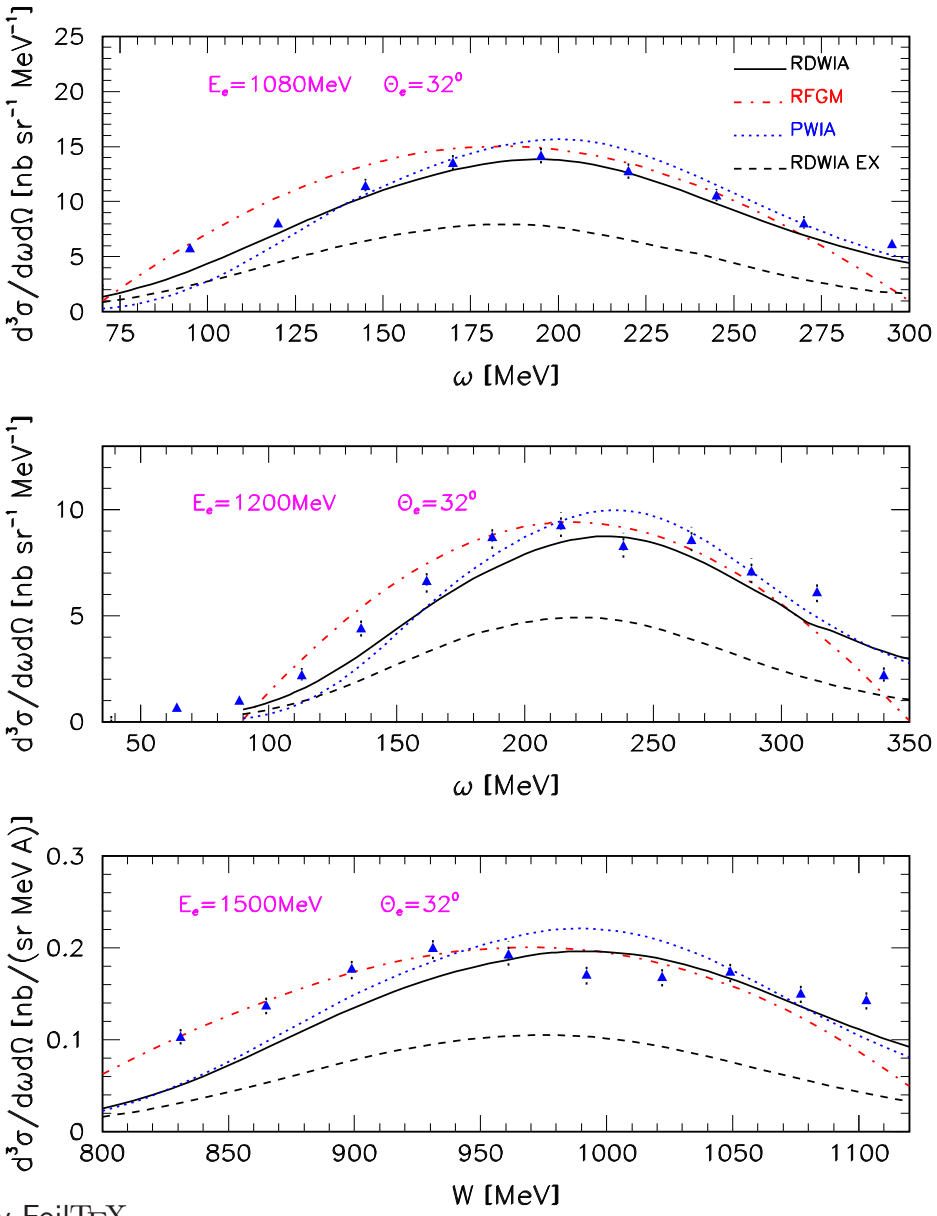

Inclusive cross section versus the energy transfer ω or invariant mass W (lower panel) for electron scattering on ^{16}O. The data are from Frascati for electron beam energy E_e=1080, 1200, and 1500 MeV and scattering angle θ=32.$^\circ$. The solid line is the RDWIA calculation while the dotted and dashed-dotted lines are respectively the PWIA and RFGM calculations. The dashed line is the cross section calculated in the RDWIA with a complex optical potential.

MiniBooNE data: $\approx 1.94 \times 10^5$ events [Phys.Rev.Lett.,100,032301,(2008)].

Flux of ν_μ neutrino is predicted with a mean energy $\sim$ 700 MeV. MC result is normalized to data. The data samples exhibit significant deficit in the region of low Q^2 $\leq$0.2 GeV^2 and small muon scattering angles which corresponds to forward going muons.

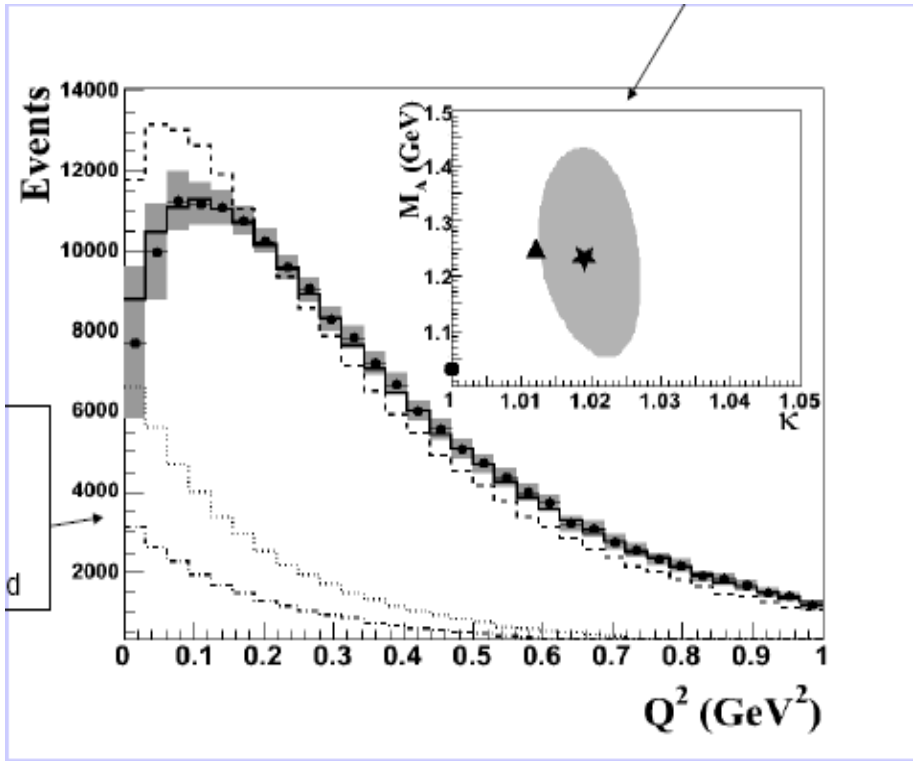

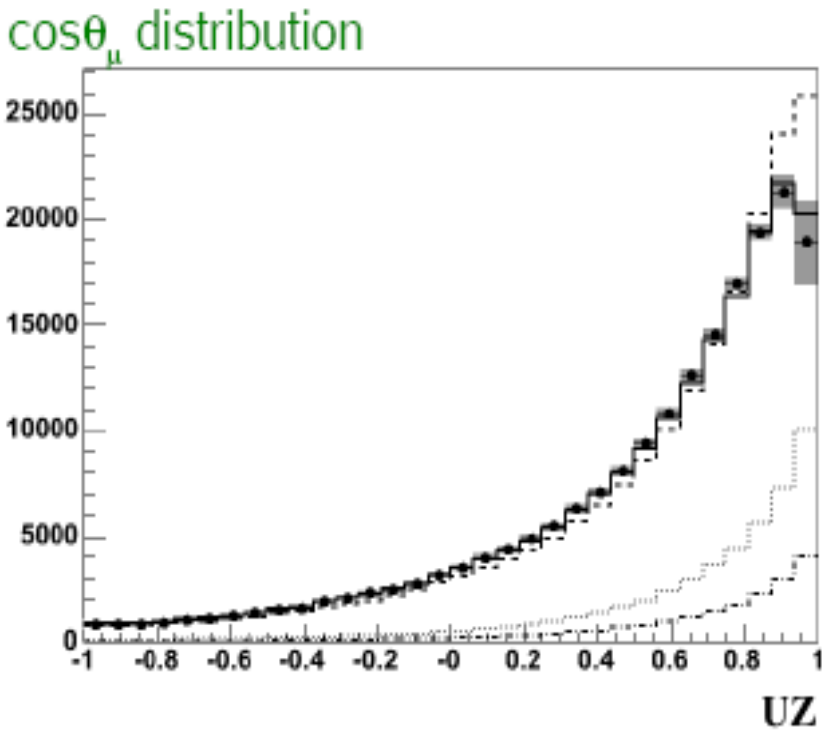

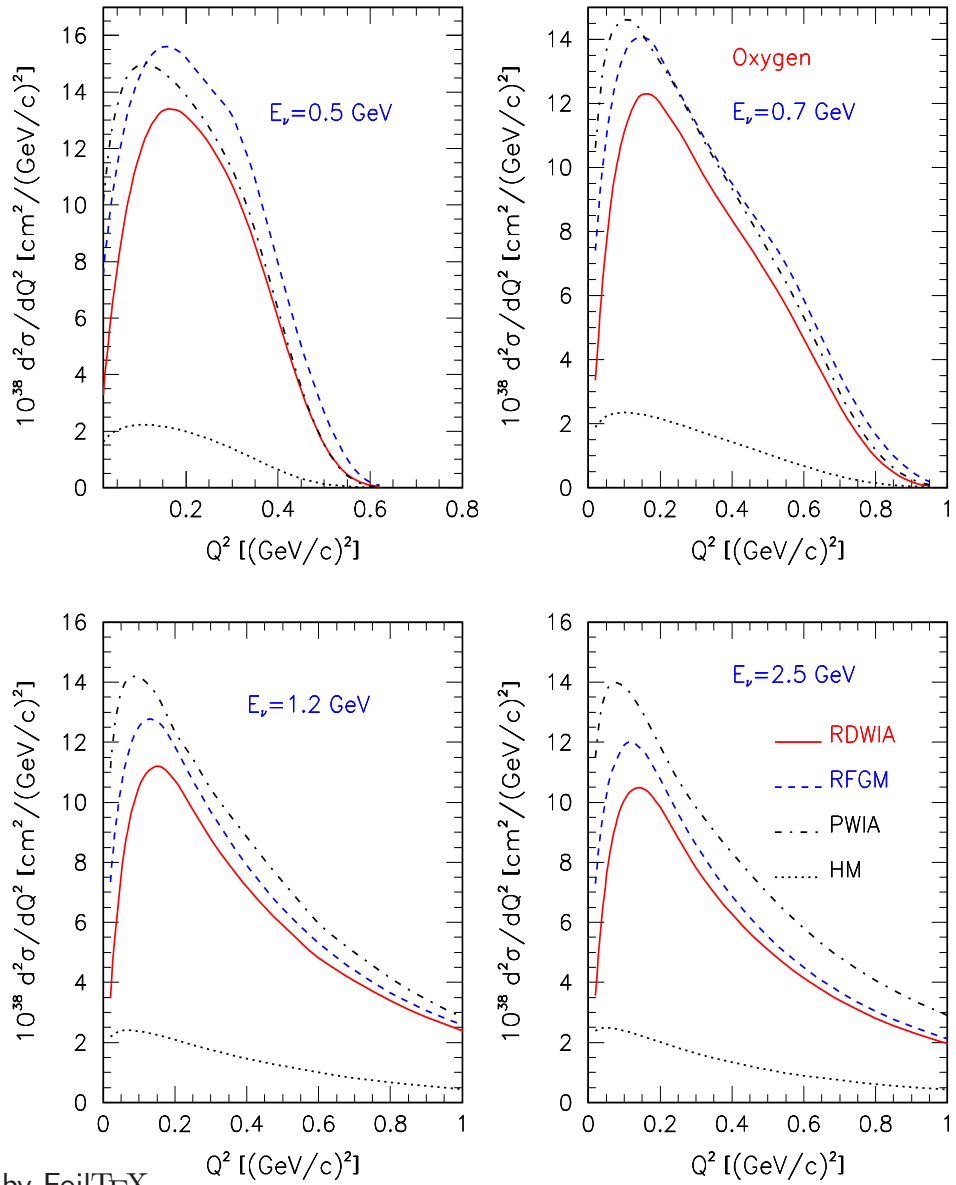

Inclusive cross section versus Q^2 for neutrino scattering on ^{16}O and for the four values of incoming neutrino energy: ε_ν=0.5, 0.7, 1.2 and 2.5 GeV. The solid line is the RDWIA calculation while the dashed and dashed-dotted lines are respectively the RFGM and PWIA calculations. The dotted line is the high-momentum component contribution to inclusive cross section. The RFGM results are higher than those obtained in the RDWIA.

In the region around the maximum $Q^2 = 0.2$ (GeV/c)^2 the difference is about $\sim 18\%$ for $\varepsilon_\nu = 0.5$ GeV and $\sim 11\%$ for $\varepsilon_\nu = 2.5$ GeV. At $Q^2 = 0.06$ (GeV/c)^2 the contribution of the HM-component increases with energy from $\sim 24\%$ up to 30% in the energy range $0.5 \div 2.5$ GeV.

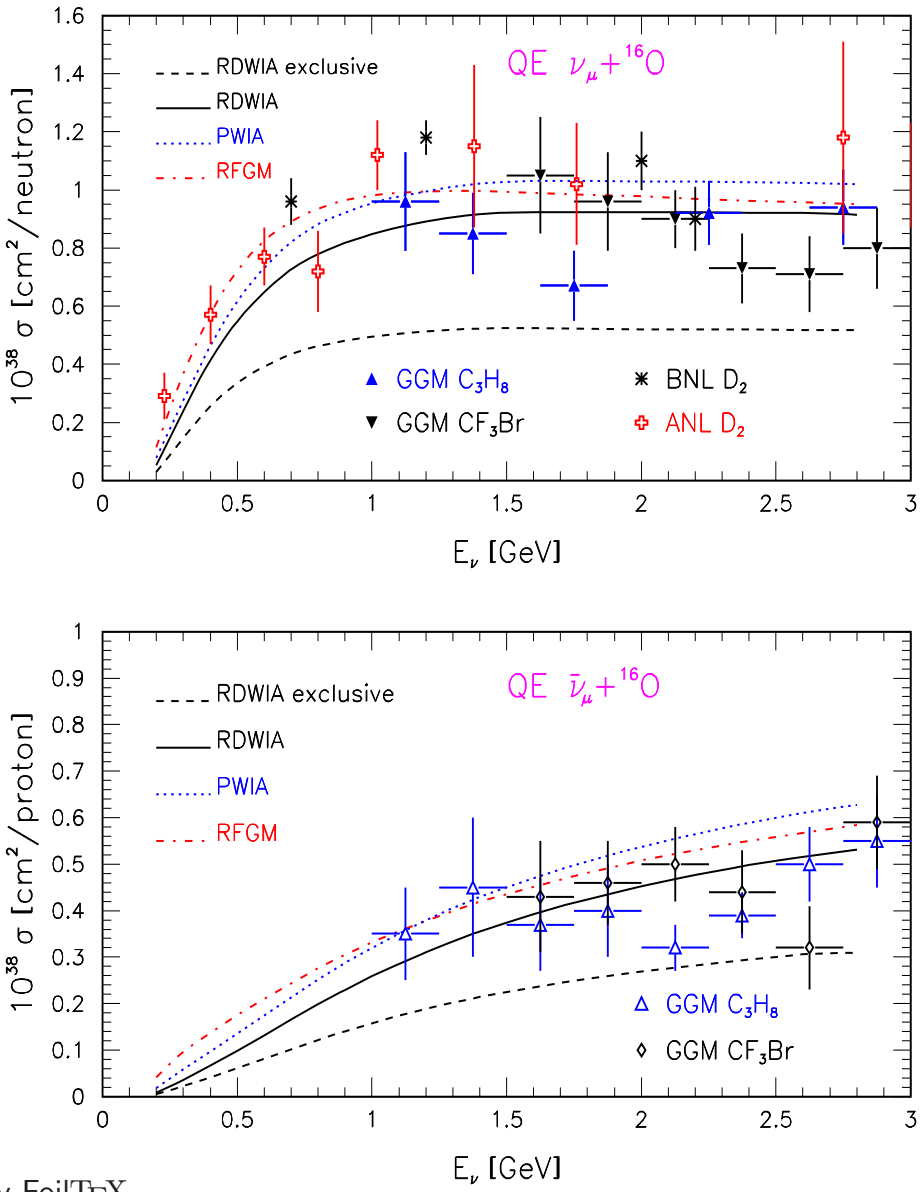

Total cross section for CC QE scattering of muon neutrino (upper panel) and antineutrino (lower panel) on ^{16}O as a function of incoming (anti)neutrino energy. The solid and dashed lines are respectively the RDWIA results with the real and complex optical potential. The dashed-dotted and dotted lines are respectively the RFGM and PWIA results. Data points for different targets are from ANL, BNL, and GGM

Neutrino energy reconstruction

CCQE scattering

- Because the CCQE interaction represent a two-particle scattering process, it forms a good signal sample, and neutrino energy may be estimated using the kinematic of this reaction.
- There are two ways to measure the neutrino energy using CCQE events: kinematic or calorimetric reconstruction.

Kinematic reconstruction method

- In detectors with the energy threshold for proton detection $\varepsilon_{th}^{p} \geq 1$ GeV (Cherenkov detectors) the muon neutrino CCQE interactions will produce the one-track events. The kinematic reconstruction is applied for these events.
- Target nucleon is in rest
  The method is based on the assumption that the target nucleon to be at rest inside the nucleus and the correlation between the incident neutrino energy and a reconstructed muon momentum and scattering angle is used in this method.

$$\varepsilon_r = \frac{\varepsilon_f(m-\epsilon_b) - (\epsilon_b^2 - 2m\epsilon_b + m_\mu^2)/2}{(m-\epsilon_b) - \varepsilon_f + k_f\cos\theta}.$$

- Nucleon Fermi motion effect

Using momentum $\boldsymbol{p}_x = \boldsymbol{p}_m + \boldsymbol{q}$ and energy balance the second order equation for neutrino energy which takes into account the bound nucleon momentum and energy distributions can be obtained.

$$A\varepsilon_r^2 - B\varepsilon_r + C = 0.$$

Now the reconstructed energy ε_r is a function of $(\boldsymbol{p}_m, \varepsilon_m, \cos\tau)$, where $\cos\tau = \boldsymbol{p}_m \cdot \boldsymbol{q}/|\boldsymbol{p}_m \cdot \boldsymbol{q}|$

- Moments of the reconstructed neutrino energy

The distribution $\varepsilon_r(\boldsymbol{p}_m, \varepsilon_m, \cos\tau)$ corresponds to measured values of $(k_f, \cos\theta)$ and at $\varepsilon_m, \boldsymbol{p}_m \longrightarrow 0$ has an asymptotic form given by the formula for nucleon at rest.
The n-th moment of $\varepsilon_r(k_f, \cos\theta, \boldsymbol{p}_m, \varepsilon_m)$ distribution versus of k_f and $\cos\theta$ can be written as

$$\langle \varepsilon_r^n(k_f, \cos\theta) \rangle = \int_{p_{min}}^{p_{max}} d\boldsymbol{p} \int_{\varepsilon_{min}}^{\varepsilon_{max}} S(\boldsymbol{p}, \varepsilon)[\varepsilon_r(k_f, \cos\theta, \boldsymbol{p}, \varepsilon)]^n d\varepsilon,$$

where $S(\boldsymbol{p}, \varepsilon)$ is the probability density function (pdf) for the target nucleon momentum and energy distribution being normalized with respect to the unit area.

- The mean of $\varepsilon_r(k_f, \cos\theta)$ and its variance $\sigma^2(\varepsilon_r)$ are defined by
$\bar{\varepsilon}_r(k_f, \cos\theta) = \langle \varepsilon_r(k_f, \cos\theta) \rangle$, $\sigma^2(\varepsilon_r) = \langle \varepsilon_r^2(k_f, \cos\theta) \rangle - \bar{\varepsilon}_r^2(k_f, \cos\theta)$

  Accuracy of reconstructed neutrino energy

- The accuracy of reconstructed energy $\varepsilon_r(\varepsilon_i)$ as a function of ε_i can be estimated using the moments of $\varepsilon_r(k_f, \cos\theta)$ distribution

$$\langle \varepsilon_r^n(\varepsilon_i) \rangle = \int dk_f \int W(k_f, \cos\theta) [\varepsilon_r(k_f, \cos\theta)]^n d\cos\theta,$$

  where $W(k_f, \cos\theta)$ is the pdf of the muon momentum and scattering angle.

- $[\varepsilon_r(k_f, \cos\theta)]^n = \langle \varepsilon^n(k_f, \cos\theta) \rangle$ if the nucleon Fermi motion effect is taken into account, or $\varepsilon_r(k_f, \cos\theta)$ is given by formula for nucleon which is at rest, if this effect is neglected.
- The reconstructed neutrino energy $\bar{\varepsilon}_r = \langle \varepsilon_r \rangle$ is smeared with variance $\sigma^2(\varepsilon_i) = \langle \varepsilon_r^2(\varepsilon_i) \rangle - \bar{\varepsilon}_r^2(\varepsilon_i)$ and biased with $\Delta(\varepsilon_i) = \varepsilon_i - \bar{\varepsilon}_r$
- The detailed description of this approach is given in [A.Butkevich PRC78:015501,(2008)].

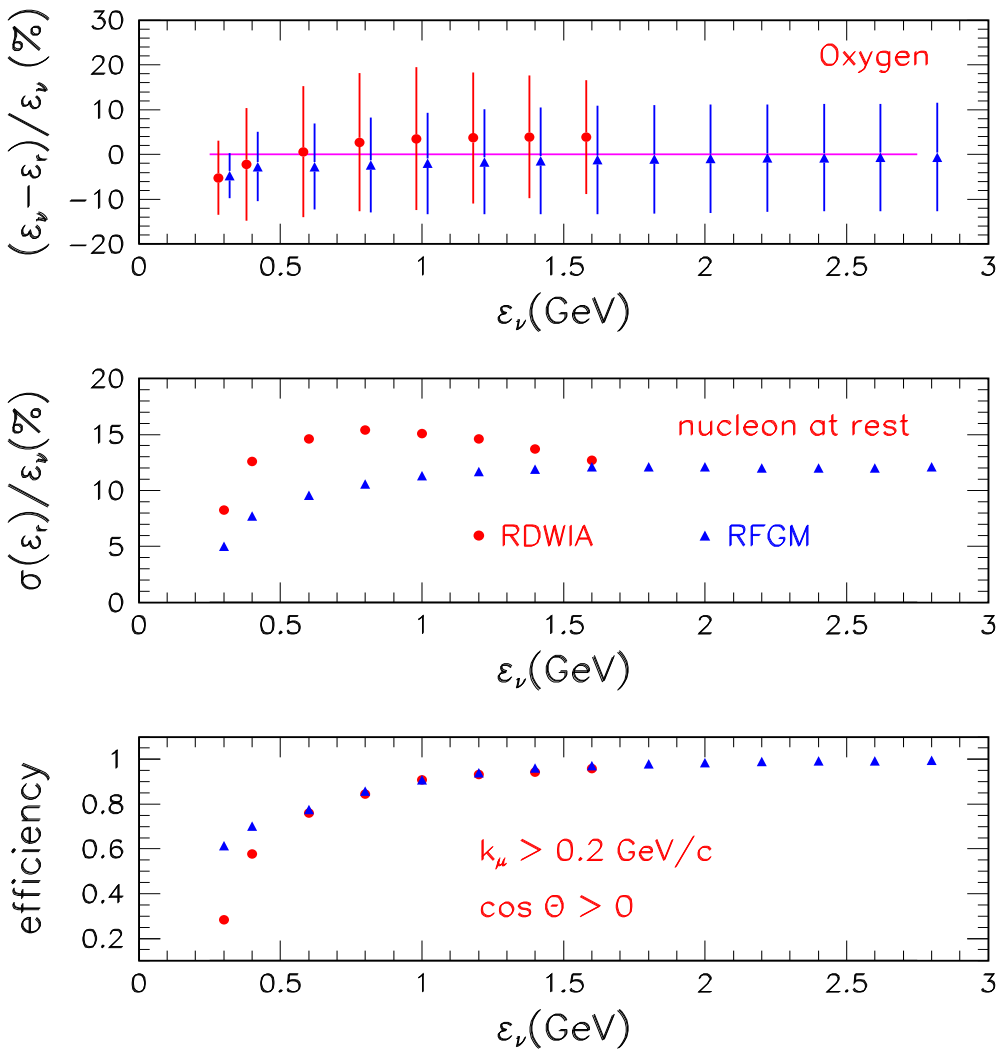

Bias (top panel), variance (middle panel) of the reconstructed neutrino energy, and efficiency (bottom panel) of the one-track events detection with $k_f \geq 0.2$ (GeV/c) and $\cos\theta \geq 0$ as functions of neutrino energy. The Neutrino energy reconstruction was formed assuming the target nucleon is at rest inside nucleus. The vertical bars show $\sigma[(\varepsilon_i - \varepsilon_r)/\varepsilon_i]$. As displayed in the key, biases, variances, and efficiencies were calculated in the RDWIA and RFGM.

RFGM: in range $0.3 \div 2.5$ $\Delta = -4.7\% \rightarrow \Delta = -0.7\%$ and $\sigma/\varepsilon_i = 5.4\% \rightarrow \sigma/\varepsilon_i = 12\%$.

RDWIA: in range $0.3 \div 1.6$ $\Delta = -5.2\% \rightarrow \Delta = 3.9\%$ and $\sigma/\varepsilon_i = 8.3\% \rightarrow \sigma/\varepsilon_i = 12.7\%$.

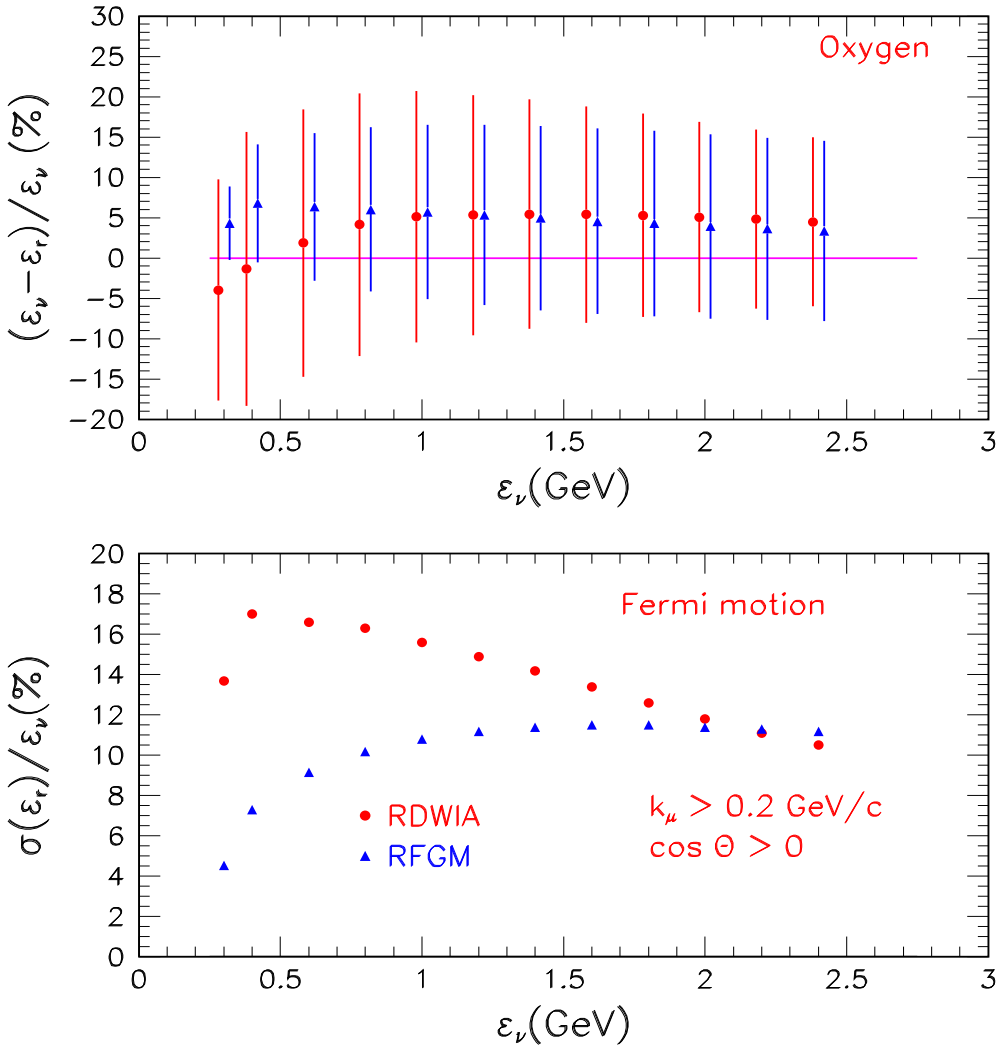

Bias (top panel) and variance (bottom panel) of the reconstructed neutrino energy as functions of neutrino energy. The energy reconstruction was formed taking into account the nucleon momentum distribution in the target with $E_{max} = 10$ GeV. As displayed in the key, biases and variances were calculated in the RDWIA and RFGM.

RFGM: in range $0.3 \div 2.5$ $\Delta = 4.3\% \rightarrow \Delta = 3\%$ and $\sigma/\varepsilon_i = 4.6\% \rightarrow \sigma/\varepsilon_i = 11\%$.

RDWIA: in range $0.3 \div 2.5$ $\Delta = -4\% \rightarrow \Delta = 4.5\%$ and $\sigma/\varepsilon_i = 14.3\% \rightarrow \sigma/\varepsilon_i = 10.5\%$.

Note: Bias may depend on the value of E_{max}.

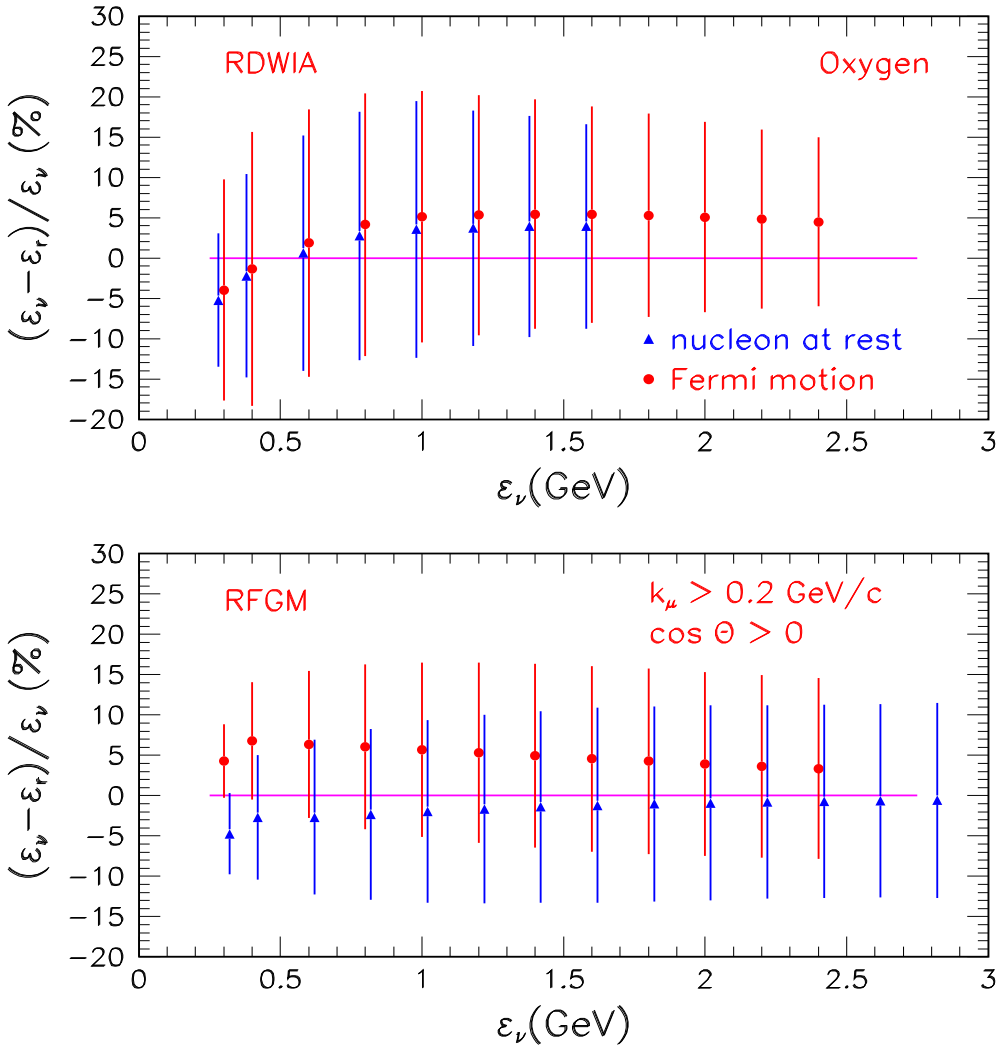

Biases calculated in the RDWIA (top panel) and RFGM (bottom panel) as functions of neutrino energy. As displayed in the key, energy reconstructions were formed with and without the nucleon momentum distribution. The biases calculated within the RDWIA and RFGM assuming that nucleon is at rest (Δ_{fr}) and using the mean energy method (Δ_{me}) are presented as functions of neutrino energy. In the RDWIA approach the nucleon Fermi motion effect leads to increase the bias by about 1.2%. In the Fermi gas model with this effect ε_r is overestimated and $\Delta_{fr}(\Delta_{me}) = -4.7\%(4.3\%)$ for energy 0.3 GeV and $\Delta_{fr}(\Delta_{me}) = -0.7\%(3.4\%)$ for $\varepsilon_\nu = 2.5$ GeV.

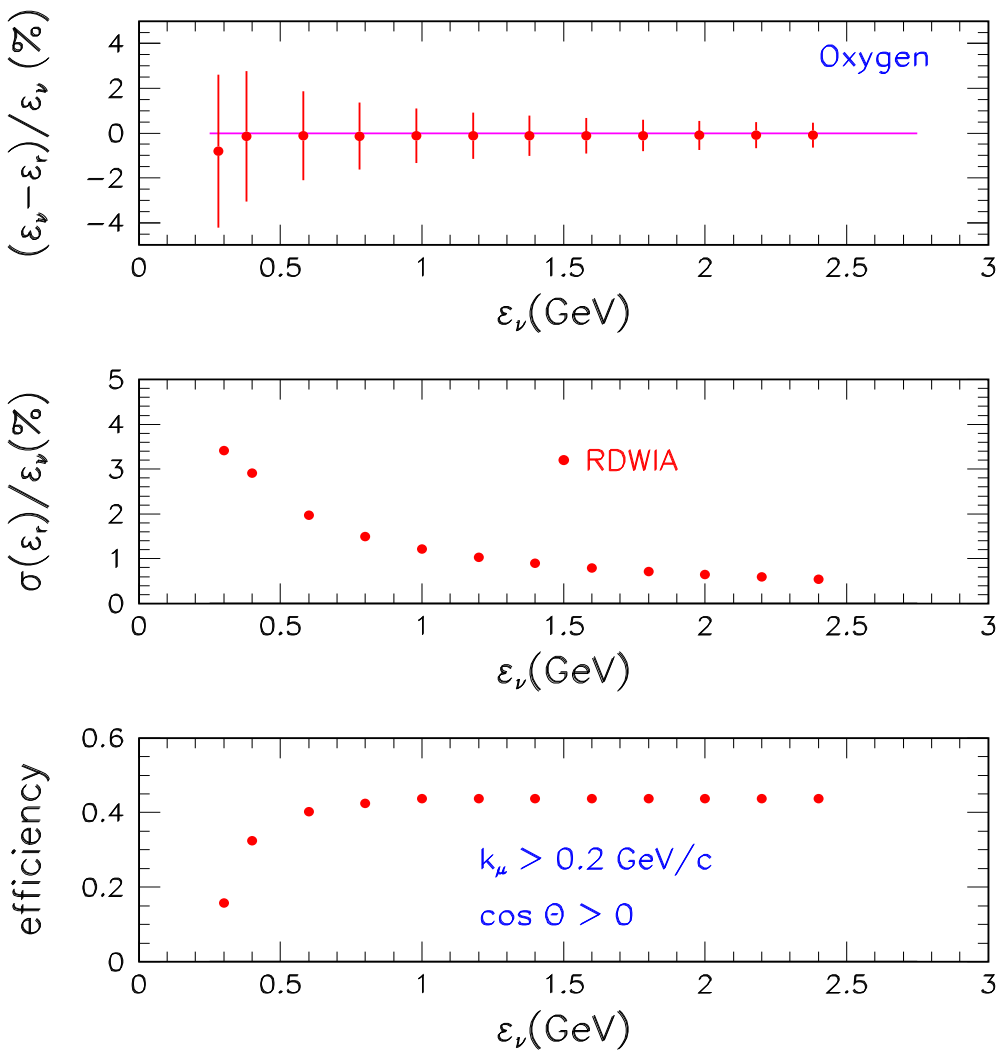

In the calorimetric reconstruction ε_r is formed as the sum of muon energy ε_f, kinematic proton energy T_p and mean missing energy $\langle\varepsilon_m\rangle$
$\varepsilon = \varepsilon_f + T_p + \langle\varepsilon_m\rangle$.
Bias (top panel), variance (middle panel) of the reconstructed neutrino energy, and efficiency (bottom panel) of the two-tracks events detection with $k_f \geq 0.2$ (GeV/c) and $\cos\theta \geq 0$ and without any cuts for proton. At $\varepsilon_\nu > 0.3$ (GeV) $\Delta = -0.1\%$. The energy resolution: 3.4% at $\varepsilon_\nu = 0.3$ (GeV) and 0.5% at $\varepsilon_\nu = 2.5$ (GeV). The challenge is identifying proton track and reconstructing its kinetic energy with reliable accuracy at low threshold energy for proton detection.

Summary

QE CC $\nu(\bar{\nu})^{16}$O cross sections were studied in different approaches.

- In RDWIA the reduced exclusive cross sections for $\nu(\bar{\nu})$ scattering are similar to those of electron scattering and in a good agreement with data.
- The inclusive and total cross sections were calculated neglecting the imaginary part of relativistic optical potential and taking into account the effect of NN-correlations in the target ground state and tested against $^{16}\mathrm{O}(e, e')$ scattering data.
- FSI effect reduces the total cross section for about 30% for $E_\nu = 200$ MeV compared to PWIA and decreases with neutrino energy down to 10% at 1 GeV.
- The Fermi gas model was tested against e^{16}O data:

  ($\star$) In the peak region RFGM overestimates the value of inclusive cross section at low momentum transfer ($|\boldsymbol{q}| < 500$ MeV/c). The discrepancy with data is about 20% at $|\boldsymbol{q}| = 300$ MeV/c and decreases as momentum transfer increases.

  ($\star$) RFGM fails completely when compared to exclusive cross section data.

  ($\star$) The calculated within the RDWIA inclusive $d^2\sigma/dQ^2$ cross sections and measured Q^2, $\cos\theta$-distributions of CCQE events reveal the inadequacies in the RFGM prediction in low Q^2 region.

- For total neutrino cross sections RFGM result is about 15% higher than the RDWIA predictions at $E_\nu \sim 1$ GeV.
- We studied the nuclear-model dependence of the energy reconstruction accuracy, neglecting by systematics related to event selection and resolution. We found that the accuracy of the kinematic reconstruction for one-track events depends on the nuclear model of CCQE neutrino interaction and neutrino energy reconstruction method.
- In the case of two-track events accuracy may be higher and does not depend on nuclear models of CCQE neutrino-nucleus interaction.